



Solid phase single-molecule counting of antibody binding to supported protein layers surface with low nonspecific adsorption

Dafeng Jiang^a, Qianqian Zhang^a, Xibo Shen^a, Lei Wang^{b,*}, Wei Jiang^{a,**}

^a School of Chemistry and Chemical Engineering, Shandong University, 250100 Jinan, PR China

^b School of Pharmacy, Shandong University, 250012 Jinan, PR China

ARTICLE INFO

Article history:

Received 14 April 2010

Received in revised form 22 May 2010

Accepted 1 June 2010

Available online 8 June 2010

Keywords:

Single-molecule counting

Supported protein layers-based surface

modification

Quantum dot

Epi-fluorescence microscopy

Antibody

ABSTRACT

On the basis of the supported protein layers (SPLs) substrate, the study presented an ultrasensitive and highly specific platform for single-molecule fluorescence detection of antibody using quantum dots (QDs) as probes. To construct the SPLs surface platform for antibody immobilization, bovine serum albumin (BSA), anti-BSA, and protein G were firstly attached to carboxyl-terminated substrate surfaces by turns. Then nonspecific adsorption of single antibody molecules on SPLs surfaces was investigated. Through the irreversible interaction between streptavidin and biotin, streptavidin-QD conjugates were employed to conjugate with biotinylated antibody, producing QD-antibody conjugates for generating fluorescent signals in fluorescent imaging. Epi-fluorescence microscopy equipped with an electron multiplying charge-coupled device was chosen as the tool for single-molecule fluorescence detection here. The concentration of antibody is quantified based on the direct counting of individual fluorescent spots, one by one. The generated fluorescent signals increased with the increasing concentration of immobilized antibody and were found to be proportional to antibody concentrations. The better brightness and photostability of QDs, and slower increase in the number of counted molecules make a large linear dynamic range of 1.0×10^{-14} to 3.0×10^{-12} mol L⁻¹ between the number of single molecules and antibody concentrations, which is comparable to the previously reported surface-based SMD analysis.

© 2010 Elsevier B.V. All rights reserved.

1. Introduction

Sensitive and specific antibody detection has attracted a strong interest in the fields of analytical chemistry, proteomics, and biomedical diagnostics [1–6]. Assays, based on the detection of disease-specific antibody in low numbers, have the ability to provide new details and insights for early-stage diagnoses [1–3]. In addition, due to the high specificity and affinity of antibodies to target analytes, antibody-based sensor technologies have found wide-ranging applications for biomolecule analysis [7–10]. Among the methods developed for more sensitive and quantitative protein analysis, single-molecule detection (SMD) methods hold great promise in this respect. SMD is accomplished by detecting the distinct fluorescent signal of single target molecules, which represents the ultimate level of sensitivity in analytical chemistry [11,12]. SMD has successfully been applied both in free solution and to surface-immobilized molecules to quantify protein analyte of ultra-low concentrations [5,13–16]. In free solution, a fluorescence signal

is detected when a fluorescence molecule diffuses into the probe volume. Due to the large diffusion rate and the short residence time of single molecules in the probe volume, it is very difficult to capture single molecules in solution with very low concentrations. Therefore, current methods for quantitative SMD analysis are largely based on protein immobilized onto a surface, employing fluorescence imaging and then counting of single target molecules [5,9,12,14,16]. Since molecules remain stationary in the fluorescence image, single-molecule counting of immobilized molecules is generally easier than that in free solution, which could eliminate the limit of either photobleaching or the residence time of the molecule on the surface by allowing signal to be integrated over time [16].

Despite recent successes, implementation of quantitative analysis using SMD method still faces several challenges. The first challenge is to minimize nonspecific adsorption yet with effective antibody immobilization on a surface. A number of efforts have been focused on obtaining functional surfaces, such as carboxyl-terminated silanization surface [14], hydrophilic layers-modified poly(dimethylsiloxane) surface [17,18], and polyelectrolyte multilayers-based membrane surface [19], to reduce nonspecific adsorption. Another common strategy for preventing nonspecific adsorption is to block the surfaces with bovine serum albumin (BSA), however, this step often hinder access of molecules

* Corresponding author. Tel.: +86 531 88382330.

** Corresponding author. Tel.: +86 531 88363888; fax: +86 531 88564464.

E-mail addresses: wangl-sdu@sdu.edu.cn (L. Wang), wjiang@sdu.edu.cn (W. Jiang).

of interest to binding sites [7,12,20–22]. Mitra and co-workers demonstrates that a BSA-coated surface has the lowest nonspecific binding among 12 evaluated surface chemistries for SMD, which still allows antibody immobilization using covalent cross-linking between them [12]. However, the abovementioned drawback still exists here and then results in a high detection limit. A second obstacle to immobilize antibody on a surface is an inevitable loss in binding affinity and poor reproducibility because of random orientation, denaturation, and chemical modification of these antibodies [23]. Due to steric problems, such as improper orientation of a fraction of the antibodies, inaccessible binding domains, or hindrance of antibody hinge motion by covalent immobilization, this loss in affinity is typically an order of magnitude or more [23,24]. To overcome these drawbacks, protein G has been used to specifically bind the Fc region of antibodies with high affinity, which is expected to better retain antibody functionality than direct covalent binding. Compared with other approaches for immobilizing protein on substrate surface (such as affinity arrays, directed antibody arrays, cell capture on a surface, etc.), the protein G-based arrays is able to form a properly oriented antibody for further antigen binding and to immobilize different types of antibodies in numerous immunoassays [5,14,17,25,26]. Recent studies have demonstrated that such immobilization methods based on specific interactions could yield oriented antibody immobilization and improve the binding capacity and sensitivity of target analytes [3,26–28]. The methods are largely based on covalent immobilization of protein G to a surface or chemical treatments of them. Therefore, the loss of biological activity of protein G is inevitable. Finally, in order to achieving high sensitivity of SMD methods (in terms of signal intensity and detection limit), the label which attached to the antibody to generate a fluorescent signal should be bright and stable [29,30].

In this study, we construct a supported protein layers (SPLs) surface for antibody immobilization with low nonspecific adsorption. Briefly, the amine groups of BSA firstly reacted with the carboxyl groups of substrate surface, generating a BSA-coated substrate surface. Then anti-BSA bound to immobilized BSA through the specific interactions between them. Finally, protein G was employed to bind on the top of the SPLs with high affinity. After that, nonspecific adsorption of single antibody molecules on the SPLs surface was first investigated. Then quantum dots (QDs), with unique optical properties, were employed to form complexes with target antibody molecules and used as fluorescent probes for single-molecule imaging [31–34]. Epi-fluorescence microscopy (EFM) was chosen as the tool for single-molecule fluorescence detection here. The generated fluorescent signals were taken by an electron multiplying charge-coupled device (EMCCD). We observed that the number of single fluorescent spots increased with the increasing concentration of antibody and was proportional to that. Under optimal conditions, this study provided a detection limit of $1.0 \times 10^{-14} \text{ mol L}^{-1}$ via a single-molecule counting approach, which was comparable to the previously reported surface-based SMD analysis.

2. Experimental

2.1. Reagents and materials

Monoclonal anti-human IgG-biotin conjugate (Clone HP-6017) was purchased from Sigma-Aldrich Co. (St. Louis, MO, USA). Qdot 605-goat F(ab')₂ anti-mouse IgG conjugate (H+L), QD 605-streptavidin conjugate and Alexa Fluor 568 labeled F(ab')₂ fragment of goat-anti-mouse IgG (H+L) were obtained from Invitrogen Co. (Eugene, OK, USA). Protein G was obtained from GenScript Co. (Piscataway, NJ, USA). Allyltrimethoxysilane (ATS) was purchased from Acros Organics BVBA (Geel, Belgium). 1-Ethyl-3-(3-dimethylaminopropyl) carbodiimide hydrochloride (EDC) and

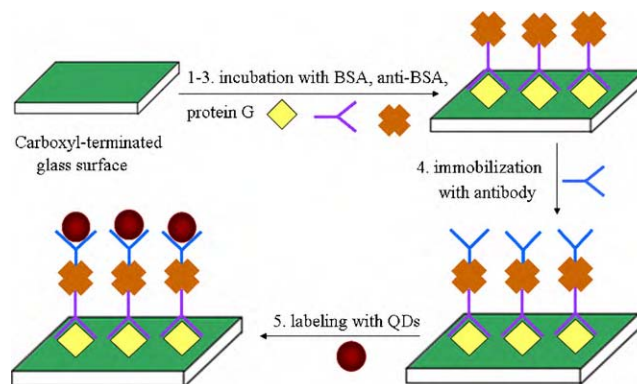


Fig. 1. Scheme for SPLs modification on the carboxyl-terminated substrate and the immobilization procedure of single QDs-labeled antibody molecules on SPLs surface.

N-hydroxysuccinimide (NHS) were obtained from Medpep Co., Ltd. (Shanghai, China). Other reagents and chemicals (analytical grade) were used as received. All buffer solutions were prepared with ultra-pure water and filtered through a 0.22 μm filter twice. Microscope cover glasses (22 mm \times 22 mm) were purchased from Cole-Parmer (IL, USA).

2.2. Apparatus

EFM imaging were performed with an Olympus IX81 fluorescence microscope (Tokyo, Japan) equipped with a high-numerical-aperture 60 \times (1.45 NA) oil-immersion objective lens, a mercury lamp source, a mirror unit consisting of a 470–490 nm excitation filter (BP470-490), a 505 nm dichromatic mirror (DM 505), a >580 nm emission filter (IF580), and a 16-bit thermoelectrically cooled EMCCD (Cascade 512B, Tucson, AZ, USA). Imaging acquisition and data analysis were performed using the MetaMorph software (Universal Imaging, Downingtown, PA, USA). The TIRFM imaging system is also equipped with a fluorescence microscope control unit, a laser incidence angle adjustment knob, and a solid laser with $\lambda = 488 \text{ nm}$ instead of a mercury lamp.

Contact angle measurement (CAM) was performed on Tensionmeter-K121 processor (Krüss Company, Germany). The glass substrates were immersed into and retracted from ultra-pure water medium. Fluorescence spectrum was taken using a Hitachi F-4500 spectrophotometer (Japan) operated at 488 nm of excitation wavelength and 10 nm of slit width. QDs at a concentration of $1.0 \times 10^{-9} \text{ mol L}^{-1}$ was measured both in phosphate buffered saline (PBS, pH 7.4) solution and borate buffer solution (pH 8.3). All measurements were performed at room temperature.

2.3. Fabrication of supported protein layers

In the procedures to form hydrophilic carboxyl-terminated substrate surfaces, the study followed the approach built in our previous work [14]. Briefly, the pretreated glasses were first dipped into 1% allyltrimethoxysilane (v/v) anhydrous toluene solution for 2 h to get the silanized surfaces. Subsequently, the vinyl-modified silanization surfaces were oxidized with permanganate-periodate ($0.5 \text{ mmol L}^{-1} \text{ KMnO}_4$, $19.5 \text{ mmol L}^{-1} \text{ NaIO}_4$, and $1.8 \text{ mmol L}^{-1} \text{ K}_2\text{CO}_3$) for 48 h with gentle stirring at room temperature. Then the substrates were rinsed with a $0.3 \text{ mol L}^{-1} \text{ NaHSO}_3$, $0.1 \text{ mol L}^{-1} \text{ HCl}$, ultra-pure water, and absolute alcohol. After that, they were dried under a nitrogen stream and stored in an oven for 20 min at 120 $^\circ\text{C}$. Finally, the glass substrates were stored in a vacuum desiccator at room temperature prior to use.

As shown in Fig. 1, the surface of carboxyl-terminated substrate was further modified by coating BSA, anti-BSA, and protein G on the top of that, which formed the SPLs surface. Briefly, the carboxyl groups were activated by a solution containing EDC (35 mg mL^{-1}) and NHS (10 mg mL^{-1}) for 2.0 h before SPLs immobilization. Then the substrate surfaces were rinsed with ultra-pure water for 120 s and dried under a nitrogen stream. For attaching the protein layers, the activated glass substrates were allowed to react with BSA for 10 h at room temperature (4 mg mL^{-1} in PBS buffer). Subsequently, the anti-BSA solution was added to incubate with the BSA through the specific interactions. At a concentration of $10 \mu\text{g mL}^{-1}$ in PBS solution, the reaction continued 6 h at room temperature. Then the substrates were incubated with protein G in PBS solution, at a concentration of $20 \mu\text{g mL}^{-1}$, the reaction continued 8 h at 37°C . For all three reactions, $100 \mu\text{L}$ of the reactant solution was used, and the glass substrates were washed with PBS and ultra-pure water for 120 s and 60 s after each step.

2.4. Antibody immobilization and QDs labeling

For the quantitative SMD analysis, monoclonal anti-human IgG-biotin conjugate was chosen as the target antibody to be detected and quantified in the experiment. First, $100 \mu\text{L}$ of the sample antibody solution with different concentrations (3.0×10^{-12} , 1.0×10^{-12} , 5.0×10^{-13} , 1.0×10^{-13} , 3.0×10^{-14} , and $1.0 \times 10^{-14} \text{ mol L}^{-1}$ in PBS buffer) were added separately in each SPLs surface. Three measurements were done for each prepared concentration. In addition, PBS solutions without the target antibody were used as the negative-control experiments. The incubation reaction proceeded for 16 h at 37°C . Subsequently, the substrate surfaces were rinsed with PBS and ultra-pure water each for 120 s and 60 s, respectively. Finally, the substrate surfaces were dried under a nitrogen stream.

QDs-streptavidin conjugates were employed to form complexes with immobilized antibody molecules and used as fluorescent probes for single-molecule imaging. They were firstly diluted in PBS solution before use. Then QDs were applied onto the antibody-immobilized SPLs surfaces. According to the instruction of the product, the dominant binding mode is one QD conjugate per analyte if the assay is carried out at a saturating concentration. In this study, corresponding to the different concentrations of target antibody, the concentrations of QDs were chosen as 10 times over the targets. This step guarantees that a single QDs molecule labeled a single immobilized antibody molecule. The reaction proceeded for 2 h at room temperature before being cleaned. Subsequently, the substrate surfaces were rinsed with PBS and ultra-pure water for 180 s and 60 s, respectively. Then, they were dried under a nitrogen stream. A borate buffer solution (pH 8.3) was placed in situ for fluorescent imaging of quantitative SMD analysis [14].

2.5. Nonspecific adsorption measurement

Nonspecific adsorption could generate false positive identifications and have an adverse effect on the accuracy and sensitivity of single-molecule counting. To quantify the efficiency of SPLs surfaces in decreasing nonspecific adsorption, two different dye-labeled antibodies, QDs-anti-mouse IgG conjugate F(ab')_2 (H+L) and Alexa Fluor 568 labeled F(ab')_2 fragment of goat-anti-mouse IgG (H+L), were added separately to the SPLs surfaces. At a concentration of $5.0 \times 10^{-12} \text{ mol L}^{-1}$, two sample antibodies incubated for 16 h at 37°C . After that, they were both rinsed with PBS and ultra-pure water for 180 s and 60 s, respectively. Finally, PBS was placed in situ for fluorescent imaging using EFM (for QDs-labeled antibody) or TIRFM (for Alexa Fluor-labeled antibody).

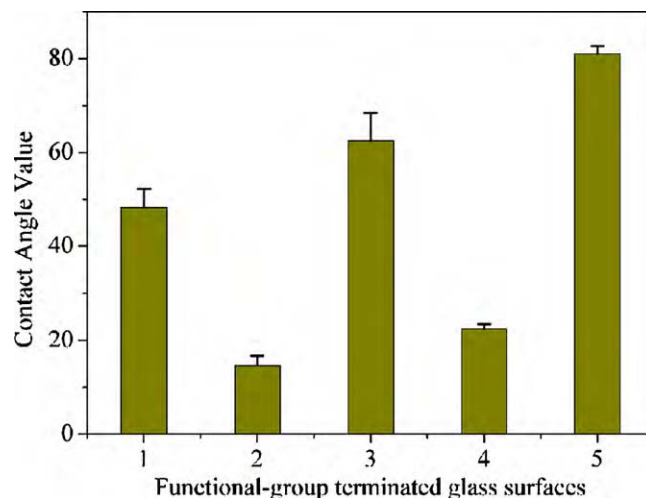


Fig. 2. CAM of the modified glass surfaces. They were characterized by measuring advancing water contact angles. The reported values for each step glass surfaces were averages and standard deviations of four measurements. Materials: 1, bare glass surface; 2, hydroxyl-group glass surface; 3, allyl-group glass surface; 4, carboxyl-group glass surface; 5, BSA-coated substrate surface.

2.6. Single-molecule imaging using EFM and TIRFM

For the fluorescent imaging of EFM, the SPLs substrate with the immobilized QDs-antibody molecules was placed on the XY sample stage. By adjusting the XY sample stage, the sample solution was moved over the $60\times$ oil-immersion objective. When the mercury lamp was switched on, excitation light of 470–490 nm passed through the excitation filter and reached the oil-immersion objective via a dichroic mirror, resulting in the excitation of the QDs-antibody complexes. The fluorescent signals of the target molecules passed through the dichroic mirror and emission filter, and were received by the EMCCD. The focus of the objective was fine-tuned until the clearest image with bright and “blinking” of fluorescent spots was observed, indicating that the strongest fluorescent signals of the target molecules immobilized on the substrate surface were detected. The fluorescent images of each location on the substrate surface were obtained by the EMCCD during the irradiation of the mercury lamp. The images corresponding to various locations were acquired by manually moving the XY sample stage. The image data were further analyzed using the MetaMorph software.

The imaging mode could be changed between EFM and TIRFM with the excitation source switched from mercury lamp to laser beam. For the TIRFM imaging, the procedure was performed according to the method described in Ref. [5]. Briefly, by adjusting the incident angle of the laser beam and the focus of the objective, the fluorescence images of TIRFM were acquired by the EMCCD. The subsequent procedures were the same as the operation of EFM.

3. Results and discussion

3.1. The hydrophilicity characterization of modified substrate surfaces

The modification of the substrate surfaces changes the terminal groups of each step on the surfaces, leading to the change of surface hydrophilicity. In this paper, CAM was employed for monitoring the surface properties of modified substrate surfaces and analyzing the hydrophilic nature of the glass surfaces. The contact angle value (CAV) of each step for the modified substrate surfaces was shown in Fig. 2. For the bare glass surface, the CAV was 48.3° , indicating a moderate hydrophilic surface. The CAV changed into 14.7°

after the activated treatment to glass substrate surfaces, which was more hydrophilic than the bare glass owing to the highly polarity of the generated hydroxyl groups. After silanization treatment, the CAV of the substrate surface increased to 62.4° . Due to the hydrophobic nature of alkane groups and non-polar vinyl groups of ATS, this procedure decreased the hydrophilicity of the substrate surface and generated hydrophobic substrate surface. The contact angle decreased with the oxidation of a vinyl group to obtain a carboxyl group, and the CAV of carboxyl-terminated surface was 22.4° . The data indicated that a hydrophilic surface with carboxyl groups was generated on the substrate surfaces, which were highly suitable for bioassays [14,17]. Finally, upon the immobilization of BSA, the CAV increased to 81.0° . The data of CAM indicates that the terminal groups with functionality were indeed generated in modified surfaces and SPLs surface was obtained on the glass substrate for antibody immobilization. In addition, the surface coverage was calculated by analyzing the area fraction (f) of the glass substrate, which was obtained following the method reported in Ref. [35]. Using the mean contact angle of the hydroxyl-group glass surface and the measured contact angle for BSA-coated substrate surface, f could be estimated to be 0.59.

3.2. Imaging analysis

For quantitative SMD analysis, the previous researches usually employ laser-induced fluorescence microscopy (LIFM) including confocal fluorescence microscopy (CFM) and TIRFM. Unlike these reported studies, EFM is utilized for single-molecule fluorescence detection here, which employs an inexpensive light source of mercury lamp and provides a convenient and alternative method for quantitative SMD analysis [14,36,37]. Additional studies were conducted to obtain the excellent resolution of single fluorescent spots in the fluorescence images by optimizing a variety of imaging conditions. In our system for fluorescent imaging, intensifier gain and exposure time were firstly selected, and the optimized values were set to 2400 and 160 ms, respectively. In this case, single fluorescent spots could be identified easily. The second step was to guarantee that the uniformity of fluorescence intensity on the images used for single-molecule counting, which aimed to overcome the limitations of the nonuniform illumination region by mercury lamp (or laser beam) through the objective. The EMCCD has an imaging region of 512×512 pixels with each pixel of $16 \mu\text{m} \times 16 \mu\text{m}$ in size. The light intensity gradually decreased from the center outward. Therefore, a 150×150 pixels subregion was selected in the method with the $60\times$ TIRFM objective and each pixel imaged $0.267 \mu\text{m} \times 0.267 \mu\text{m}$ in the object plane. Thus, the subframe image with an area of $40 \mu\text{m} \times 40 \mu\text{m}$ was used for single-molecule counting. For each concentration, 60 (three images of each location) subframe images were obtained from location to location on the substrate surface by moving the XY sample stage.

3.3. Nonspecific adsorption and the estimation of detection limit

Nonspecific adsorption could generate false positive identifications and have an adverse effect on the accuracy and sensitivity of quantitative SMD analysis. Therefore, it is critical to minimize the nonspecific adsorption of antibodies to solid surfaces for the development of single-molecule immunoassays [12]. The silanized surfaces are often hydrophobic as a result of their hydrophobic chains, which are liable to cause protein adsorption owing to the hydrophobic interaction between them and the hydrophobic domains of proteins. In this study, we first provide a hydrophilic environment by generating the carboxyl-terminated silanized surface, which is highly suitable for bioassays. Subsequently, BSA, a common used blocking agent, is employed here to reduce nonspecific binding. Finally, anti-BSA and protein G are incubated with the

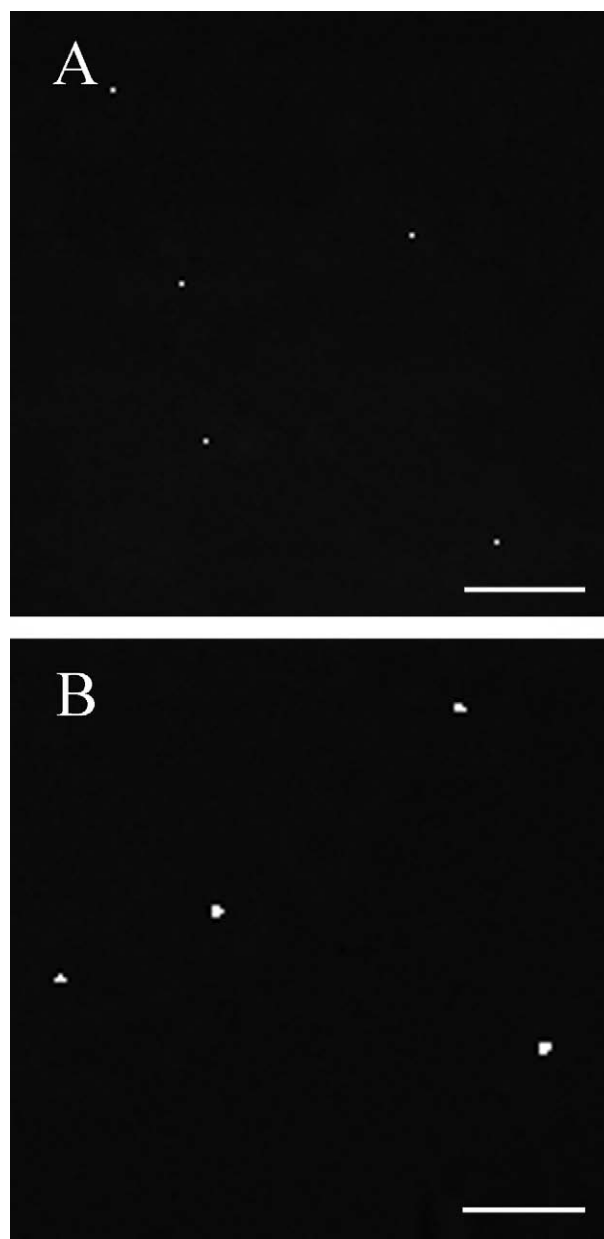


Fig. 3. The quantitative SMD analysis of nonspecific adsorption on SPLs substrate surfaces after incubation with dye-labeled antibody at a concentration of $5.0 \times 10^{-12} \text{ mol L}^{-1}$: (A) fluorescent image of Alexa Fluor-labeled antibody by TIRFM; (B) fluorescent image of QDs-labeled antibody by EFM. Scale bar, $8 \mu\text{m}$. Image conditions for TIRFM: excitation wavelength, 488 nm; emission wavelength, $>580 \text{ nm}$; readout speed, 5 MHz. Image conditions for EFM: excitation wavelength, 470–490 nm; emission wavelength, $>580 \text{ nm}$; readout speed, 5 MHz.

BSA-immobilized surface by turns, which form the SPLs surface. To quantify the efficiency of the SPLs surface in decreasing nonspecific adsorption, a study quantified the nonspecific adsorption of dye-labeled antibodies via a single-molecule counting approach was conducted. In order to eliminate the effects caused by different kinds of fluorescent probes, both Alexa Fluor-labeled antibody (organic dye-labeled antibody conjugate) and QDs-labeled antibody (inorganic dye-labeled antibody conjugate) were used for investigating nonspecific adsorption. Fluorescent images of SPLs surfaces after incubating with different dye-labeled antibodies were shown in Fig. 3A and B, respectively. At a concentration of $5.0 \times 10^{-12} \text{ mol L}^{-1}$ for each dye-labeled antibody, it is obvious that only a few fluorescent spots are observed on the SPLs surfaces.

For Alexa Fluor-labeled antibody fragment, only 537 spots were observed in 100 images, i.e., about 5.4 spots appeared in an image on average. For QDs-labeled antibody fragment, only 375 spots were observed in 100 images, i.e., about 3.8 spots appeared in an image on average. The number of nonspecific adsorption was similar for two different dye-labeled antibodies, which indicated that the types of fluorescent probes had no effect on antibody adsorption. Both results demonstrated that there was only a few number of adsorbed antibody molecules on the SPLs surfaces. Thus, we can conclude that the number of the nonspecifically bounded antibody was extremely small on fabricated SPLs surfaces at a level of the concentrations below $5.0 \times 10^{-12} \text{ mol L}^{-1}$.

In the negative-control experiments, QDs-streptavidin conjugates could not be adsorbed on the SPLs surfaces, since protein G on the top of SPLs surfaces only react with the Fc terminal of biotinylated antibody. After a clean step with PBS and ultra-pure water, the free QDs were easily rinsed off from the substrate surfaces. For the detection limit estimate, it depends on the number of subframe images that are used for count. To quantify the concentration of fluorescent spots in a solution of very low concentration, we should acquire as many images on substrate surfaces as possible. When 20 images were acquired here and ensured that the molecule number in positive experiments was at least two times as many as that in negative-control ones, the detection limit was down to $1.0 \times 10^{-14} \text{ mol L}^{-1}$ with a single-molecule counting approach.

3.4. The effect of QDs for fluorescent imaging and the identification of single spots

In this study, QDs-streptavidin conjugate is employed to form complexes with biotinylated antibody molecules and used as fluorescent label for single-molecule imaging. Through the irreversible interaction between streptavidin and biotin ($K_a = 10^{15} \text{ mol L}^{-1}$) with rapid binding kinetics and strong affinity, this procedure leads to stable QDs-labeled antibody complex. For fluorescent imaging, a variety of photophysical effects relating to QDs were considered in this experiment. Firstly, it is found that on continuous excitation, the photoluminescence intensity of QDs initially increases and converges to a maximum value. Therefore, the irradiation of the light continued 60–90 s for each location of the substrate surfaces, and fluorescent images for different location were acquired by the EMCCD during this time. Secondly, most available QDs to date still suffer from photoblinking of single QDs. This fluorescence intermittency (blinking between on and off state) is a potential limitation of QDs for single-molecule counting, since that only QDs that are in the ON state in the detection volume at the time of acquisition will be detected. In other words, a fluorescent signal of single QD may be not appear in the images when it is imaged in the OFF state. To eliminate the effect of the “blinking” and improve the accuracy of single-molecule counting, three images were obtained during the irradiation of the light in the same location. During the subsequent data analysis, the average number of fluorescent spots in three subframe images was taken as the number of the single molecules in the location. Finally, the fluorescence intensities of QDs both in PBS buffer solution and in borate buffer solution were investigated. QDs maintained good spectral emission in both buffer solutions, but the fluorescence intensity of them in borate buffer solution was higher than that in the PBS buffer solution (data not shown here). Therefore, borate buffer solution was selected for the final fluorescence imaging of QD-antibody conjugates immobilized on the SPLs surface.

As discussed above, the blinking of QDs is a limitation for fluorescent imaging, however, this phenomenon can be utilized for the identification of single QDs. In other words, this indicates the presence of a single QD in the SPLs surfaces. Corresponding to the different concentrations of immobilized antibody, the concentra-

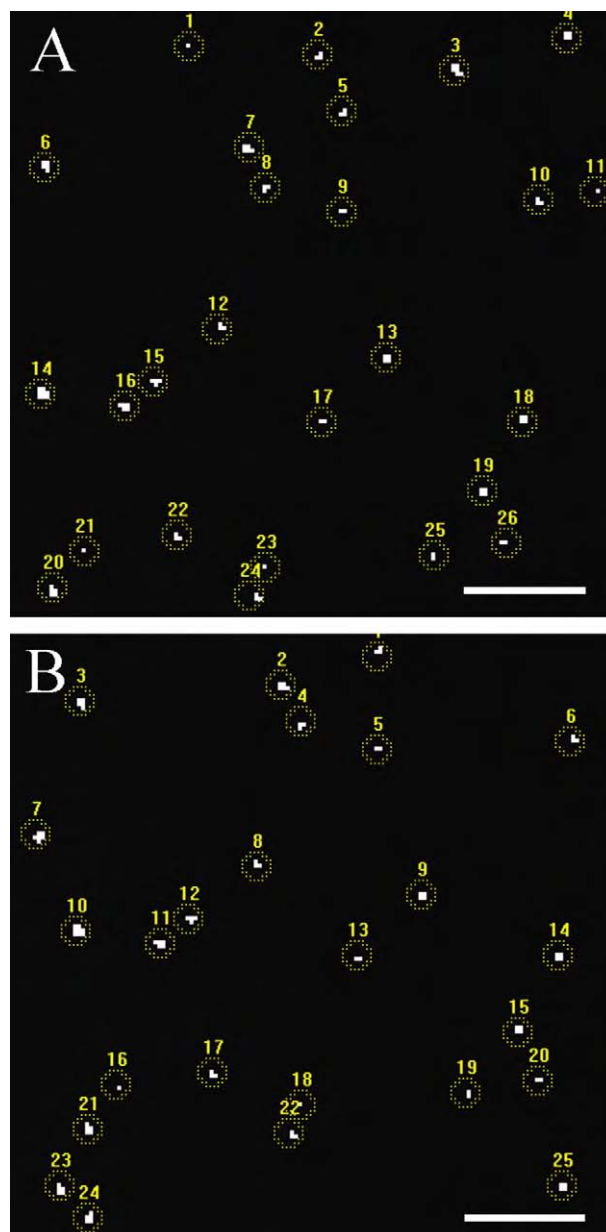


Fig. 4. The typical 3 times amplification subframe images for the pixel area of single fluorescent spots at the $5.0 \times 10^{-13} \text{ mol L}^{-1}$ positive experiments. Scale bar, 8 μm . Image conditions for EFM: excitation wavelength, 470–490 nm; emission wavelength, $>580 \text{ nm}$; readout speed, 5 MHz.

tions of QDs were chosen as 10 times over the targets here. This concentration ratio of QDs to target antibody molecules guaranteed that a single QDs molecule labeled a single immobilized antibody molecule. Therefore, a single fluorescent spot corresponded to a single antibody molecule in fluorescent images. For a further step, the fluorescence intensities of individual spots are analyzed. The abovementioned two factors are considered before analyze: (1) the available QDs suffers from the blinking (ON/OFF) of single QDs; (2) on continuous excitation, the photoluminescence intensity of QDs initially increases and converges to a maximum value. This two factors result in the different fluorescence intensity of individual QDs. Therefore, the shape of individual spots is difference, meaning that single fluorescent spots occupy different pixel area above the optimal threshold. As shown in Fig. 4, the pixel intensity of single QD does not exceed a 3×3 pixel area in the images. A statistical research of the size across 500 spots at $5.0 \times 10^{-13} \text{ mol L}^{-1}$ positive

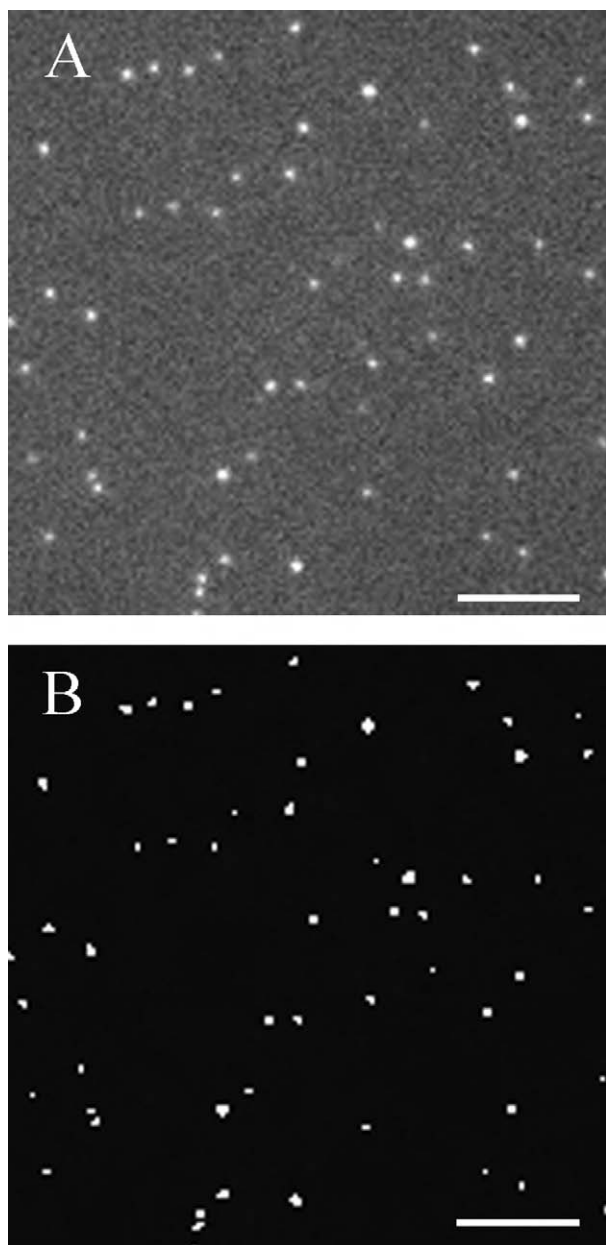


Fig. 5. A typical subframe image of fluorescent spots for immobilized antibody molecules at a concentration of $1.0 \times 10^{-12} \text{ mol L}^{-1}$. Images show before (A) and after (B) setting the optimal threshold. Scale bar, $8 \mu\text{m}$. Other conditions as in Fig. 4.

experiments demonstrates that the pixel intensities of nearly all (>96.5%) single fluorescence spots are no more than this pixel area of a single QDs. The results indicate that the fluorescent spots are single QDs in the subframe images.

3.5. The selection of threshold and the quantification of antibody

As discussed above, single fluorescent spots corresponded to single antibody molecules. A typical subframe image of fluorescent spots for positive experiment at a concentration of $1.0 \times 10^{-12} \text{ mol L}^{-1}$ was shown in Fig. 5A. It is obvious that single fluorescent spots could be distinguished from background noise in the subframe image. However, the fluorescence intensities of single spots were different and the contrast between single fluorescent spots and background noise was not striking. In order to solve this problem and ensure the accuracy and reproducibility of the results

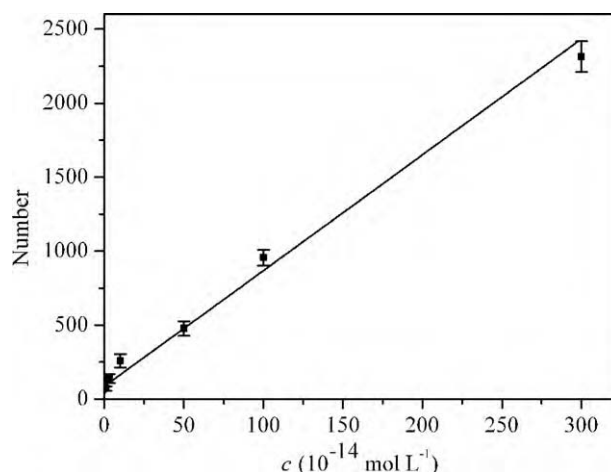


Fig. 6. Relationship between the number of single molecules and antibody concentration. Conditions as in Fig. 4.

for quantitative SMD analysis, the acquired subframe images need to be further processed. In other words, it was necessary to optimize the threshold for the elimination of background noise to improve the performance of single-molecule counting. A reported strategy in our previous work was adopted to obtain suitable threshold here [14]. Briefly, 15 different threshold values corresponding to 15 different subframe images of blank SPLs surfaces were applied to remove background noise, which mainly consists of buffer background fluorescence and associated noise. Then the mean value and standard deviation (σ) of 15 threshold values were calculated. The optimized threshold was defined as 3σ above the mean value for the identification of the fluorescent spots. After the optimal threshold was set, we further defined target molecules as sets of pixels that (1) have intensity values are greater than the threshold, (2) are contiguous with other pixels within that spot and (3) comprise an area within 3×3 pixel. Nearly all spots on the subframe images in lower concentrations ($\leq 5.0 \times 10^{-13} \text{ mol L}^{-1}$) satisfied with the conditions, meaning that single spots corresponded to single target molecules. Only few spots in higher concentrations occupied more than 3×3 pixel area, which exceeded that of a single molecule. The higher the concentration, the more spots there were that occupied larger pixel area. In these cases, taking the ratio of the larger area in the subframe images to the average pixel area of a single molecule as the number of single molecules is more accurate than taking the number of single fluorescence spots, even if the calibration is somewhat rough. The typical subframe image of fluorescent spots for positive experiment after the selection of threshold was shown in Fig. 5B, which was obtained from the same location as shown in Fig. 5A.

To quantify the antibody, the numbers of fluorescent spots in 720 subframe images of all positive and negative-control experiments over a concentration region of 1.0×10^{-14} to $3.0 \times 10^{-12} \text{ mol L}^{-1}$ are analyzed and counted. The approach is general and is based on the direct counting of individual antibody labeled with QD on the SPLs surfaces, molecule by molecule, without any amplification steps. The number of QDs increased with the increasing concentration of immobilized antibody on SPLs surfaces. For each concentration of the sample solution, the total number of single molecules in each subframe image was obtained. The molecule number corresponding to an antibody concentration was calculated via the total molecule number in positive experiments subtracted that in negative-control ones. The reported numbers of each concentration are the averages of three-time measurements under the same optimal condition. As shown in Fig. 6, the linear relationship between the antibody concentration and the

number of molecules was obtained in the range of 1.0×10^{-14} to 3.0×10^{-12} mol L⁻¹, the coefficient correlation was 0.9920. The relative standard deviation (RSD) was 5.7% for the concentration of 1.0×10^{-12} mol L⁻¹ ($n=3$). The low background level, the better brightness and photostability of QDs, and slower increase in the number of counted molecules make the linear dynamic range much large.

4. Conclusions

This article describes a platform of SPLs surface for oriented antibody immobilization with low nonspecific adsorption, providing a promising method for the development of ultrasensitive immunoassays. Owing to the improved brightness and photostability achieved by employing QDs as fluorescent probe and oriented antibody conjugation with protein G on the top of SPLs surface, counting of single target molecules has been realized. The concentration of antibody is quantified based on the direct counting of individual fluorescent spots, molecule by molecule, without the need for any amplification technique. The number of fluorescent spots increased with the increasing concentration of antibody immobilized on SPLs surfaces, and slower increase in the number of counted molecules make a large linear dynamic range. The method provided a limit of detection at 1.0×10^{-14} mol L⁻¹, which is comparable to the previously reported surface-based SMD analysis. For the following work in future, the successful fabrication of SPLs surface and the low detection limit of the method suggest that it can be a promising strategy in detection of proteins at femtomolar level by sandwich immunoassays.

Acknowledgements

This project was supported by the National Natural Science Foundation of China (Grant Nos. 20775043, 20875056) and the Natural Science Foundation of Shandong Province in China (Grant No. Z2008B05).

References

- [1] K.E. Sapsford, J.B. Blanco-Canosa, P.E. Dawson, I.L. Medintz, *Bioconjug. Chem.* 21 (2010) 393–398.
- [2] P. Waters, A. Vincent, *Int. MS J.* 15 (2008) 99–105.
- [3] D. Gao, N. McBean, J.S. Schultz, Y. Yan, A. Mulchandani, W. Chen, *J. Am. Chem. Soc.* 128 (2006) 676–677.
- [4] Y. Jung, H.J. Kang, J.M. Lee, S.O. Jung, W.S. Yun, S.J. Chung, B.H. Chung, *Anal. Biochem.* 374 (2008) 99–105.
- [5] D. Jiang, L. Wang, W. Jiang, *Anal. Chim. Acta* 634 (2009) 83–88.
- [6] S.Y. Tetin, S.D. Stroupe, *Curr. Pharm. Biotechnol.* 5 (2004) 9–16.
- [7] W. Liang, W. Yi, S. Li, R. Yuan, A. Chen, S. Chen, G. Xiang, C. Hu, *Clin. Biochem.* 42 (2009) 1524–1530.
- [8] J.P. Kim, B.Y. Lee, J. Lee, S. Hong, S.J. Sim, *Biosens. Bioelectron.* 24 (2009) 3372–3378.
- [9] S. Lee, S. Lee, Y.H. Ko, H. Jung, J.D. Kim, J.M. Song, J. Choo, S.K. Eo, S.H. Kang, *Talanta* 78 (2009) 608–612.
- [10] M.A. Hahn, J.S. Tabb, T.D. Krauss, *Anal. Chem.* 77 (2005) 4861–4869.
- [11] S. Weiss, *Science* 283 (1999) 1676–1683.
- [12] L.A. Tessler, J.G. Reifenger, R.D. Mitra, *Anal. Chem.* 81 (2009) 7141–7148.
- [13] A. Agrawal, C. Zhang, T. Byassee, R.A. Tripp, S. Nie, *Anal. Chem.* 78 (2006) 1061–1070.
- [14] D. Jiang, C. Liu, L. Wang, W. Jiang, *Anal. Chim. Acta* 662 (2010) 170–176.
- [15] H. Li, D. Zhou, H. Browne, S. Balasubramanian, D. Klenerman, *Anal. Chem.* 76 (2004) 4446–4451.
- [16] E.M. Peterson, J.M. Harris, *Anal. Chem.* 82 (2010) 189–196.
- [17] W.C. Sung, C.C. Chang, H. Makamba, S.H. Chen, *Anal. Chem.* 80 (2008) 1529–1535.
- [18] W.C. Sung, H.H. Chen, H. Makamba, S.H. Chen, *Anal. Chem.* 81 (2009) 7967–7973.
- [19] J. Dai, G.L. Baker, M.L. Bruening, *Anal. Chem.* 78 (2006) 135–140.
- [20] Q. Zhang, L.H. Guo, *Bioconjug. Chem.* 18 (2007) 1668–1672.
- [21] Q. Ma, T.Y. Song, P. Yuan, C. Wang, X.G. Su, *Colloid Surf. B: Biointerfaces* 64 (2008) 248–254.
- [22] H. Wang, J. Wang, C. Timchalk, Y. Lin, *Anal. Chem.* 80 (2008) 8477–8484.
- [23] J.P. Temirov, A.R. Bradbury, J.H. Werner, *Anal. Chem.* 80 (2008) 8642–8648.
- [24] R.A. Vijayendran, D.E. Leckband, *Anal. Chem.* 73 (2001) 471–480.
- [25] R. Hurst, B. Hook, M.R. Slater, J. Hartnett, D.R. Storts, N. Nath, *Anal. Biochem.* 392 (2009) 45–53.
- [26] Y. Jung, J.M. Lee, H. Jung, B.H. Chung, *Anal. Chem.* 79 (2007) 6534–6541.
- [27] Y. Jung, J.M. Lee, J.W. Kim, J. Yoon, H. Cho, B.H. Chung, *Anal. Chem.* 81 (2009) 936–942.
- [28] J.M. Lee, H.K. Park, Y. Jung, J.K. Kim, S.O. Jung, B.H. Chung, *Anal. Chem.* 79 (2007) 2680–2687.
- [29] C. Xie, F. Xu, X. Huang, C. Dong, J. Ren, J. Am. Chem. Soc. 131 (2009) 12763–12770.
- [30] G. Rousserie, A. Sukhanova, K. Even-Desrumeaux, F. Fleury, P. Chames, D. Baty, V. Oleinikov, M. Pluot, J.H. Cohen, I. Nabiev, *Crit. Rev. Oncol. Hematol.* 74 (2010) 1–15.
- [31] H.M. Azzazy, M.M. Mansour, S.C. Kazmierczak, *Clin. Biochem.* 40 (2007) 917–927.
- [32] T. Jamieson, R. Bakhshi, D. Petrova, R. Pocock, M. Imani, A.M. Seifalian, *Biomaterials* 28 (2007) 4717–4732.
- [33] I.L. Medintz, H.T. Uyeda, E.R. Goldman, H. Mattoussi, *Nat. Mater.* 4 (2005) 435–446.
- [34] K. Kerman, T. Endo, M. Tsukamoto, M. Chikae, Y. Takamura, E. Tamiya, *Talanta* 71 (2007) 1494–1499.
- [35] K. Liu, Y. Tian, R. Pitchimani, M. Huang, H. Lincoln, D. Pappas, *Talanta* 79 (2009) 333–338.
- [36] R. Han, Y. Zhang, X. Dong, H. Gai, E.S. Yeung, *Anal. Chim. Acta* 619 (2008) 209–214.
- [37] D.C. Hanley, J.M. Harris, *Anal. Chem.* 73 (2001) 5030–5037.